Published in final edited form as:
Biomaterials. 2014 August ; 35(25): 6850–6858. doi:10.1016/j.biomaterials.2014.04.114.

Comparison of biomaterial delivery vehicles for improving acute retention of stem cells in the infarcted heart

Ellen T. Roche[#1,2], **Conn L. Hastings**[#3,4,5], **Sarah A. Lewin**[2], **Dmitry Shvartsman**[1,2], **Yevgeny Brudno**[1,2], **Nikolay V. Vasilyev**[6], **Fergal J. O'Brien**[3,4,5], **Conor J. Walsh**[1,2], **Garry P. Duffy**[3,4,5], and **David J. Mooney**[1,2,*]

[1]School of Engineering and Applied Sciences, Harvard University, 29 Oxford street, Cambridge, MA 02138, USA [2]Wyss Institute for Biologically Inspired Engineering, 60 Oxford street, Cambridge, MA 02138, USA [3]Tissue Engineering Research Group, Dept. of Anatomy, Royal College of Surgeons in Ireland (RCSI), 123 St. Stephens Green, Dublin 2, Ireland [4]Trinity Centre for Bioengineering, Trinity College Dublin (TCD), College Green, Dublin 2, Ireland [5]Advanced Materials and Bioengineering Research (AMBER) Centre, RCSI & TCD, Dublin 2, Ireland [6]Boston Children's Hospital, 300 Longwood Avenue, Boston, MA 02115, USA

[#] These authors contributed equally to this work.

Abstract

Cell delivery to the infarcted heart has emerged as a promising therapy, but is limited by very low acute retention and engraftment of cells. The objective of the study was to compare a panel of biomaterials to evaluate if acute retention can be improved with a biomaterial carrier. Cells were quantified post-implantation in a rat myocardial infarct model in five groups (n=7–8); saline injection (current clinical standard), two injectable hydrogels (alginate, chitosan/β-glycerophosphate) and two epicardial patches (alginate, collagen). Human mesenchymal stem cells (hMSCs) were delivered to the infarct border zone with each biomaterial. At 24 hours, retained cells were quantified by fluorescence. All biomaterials had superior fluorescence to saline control, with 8 and 14-fold increases with alginate and chitosan/β-GP injectables, and 47 and 59-fold increases achieved with collagen and alginate patches, respectively. Immunohistochemical analysis qualitatively confirmed these findings. All four biomaterials retained 50–60% of cells that were present immediately following transplantation, compared to 10% for the saline control. In conclusion, all four injectable hydrogels and epicardial patches were demonstrated to more efficiently deliver and retain cells when compared to a saline control. Biomaterial-based delivery approaches show promise for future development of efficient *in vivo* delivery techniques.

[*]Corresponding Author Professor David Mooney Pierce Hall Room 319, 29 Oxford Street, Cambridge, MA 02138 USA Phone: +1 617 384-9624 Fax: +1 617 495-9837 mooneyd@seas.harvard.edu.

Disclosures None

Introduction

In the US one person suffers a myocardial infarction (MI) every 34 seconds [1]. As a result, approximately one million people are discharged from hospital with heart failure annually [1]. With advancements in the acute treatment of myocardial infarction death rates have improved dramatically, but strategies for treating those who go on to develop ventricular dysfunction are lacking. Stem cell therapy is a promising candidate for treatment of acute myocardial infarction and ischemic cardiomyopathy. One of the major hurdles in successful clinical translation of cardiac cell therapy is poor cell survival, retention and engraftment in the infarcted heart – a critical requirement for effective treatment. Tissue retention of cells is persistently low. Various factors contribute to this phenomenon and include exposure of cells to ischemia and inflammation, mechanical washout of cells from incessantly beating myocardium, flushing by the coronary vasculature, leakage of cell suspension from the injection site and anoikis [2–4]. The overwhelming majority of cell displacement and death occurs within the first few days after delivery. Therefore, an early assessment of cell retention is likely to be strongly predictive of longer-term retention and engraftment [4]. Reported rates of cell retention in animal hearts, where cells were administered intramyocardially as a simple suspension in saline (the current clinical standard) or media, vary with administered cell type and cell number, along with the time of analysis post-delivery and the time of delivery post-MI. However, retention is typically very poor. For example, delivery of mesenchymal stem cells (MSCs) to infarcted rat or porcine hearts in the manner described above (media/saline suspension, intramyocardial injection) has yielded results as low as 11% retention at 90 minutes and 0.6% retention at 24 hours [5–7]. Studies in human subjects confirm the low retention phenomenon [8,9]. Regardless of cell type or delivery route, acute retention of less than 10% is generally reported with saline/media. Studies with different cell types show a strong correlation between engraftment rate and long-term functional benefit [10–12] supporting the hypothesis that new strategies to improve delivery and engraftment of cells could increase therapeutic benefit.

The development of cell therapy as a feasible therapeutic option in the treatment of myocardial infarction (MI) is in part dependent on new strategies to enable viable cells to remain in infarcted tissue and exert therapeutic benefit for extended periods. Investigated strategies have included efforts to manipulate the cells themselves, such as induction of pro-survival signals through heat-shock or transduction of administered cells with pro-survival factors like Bcl-2 [4,13]. However, these interventions do not directly address the physical factors which result in dispersion of cells or anoikic death as a result of poor attachment site presentation. An alternative is to utilize a biomaterial approach, whereby a biomaterial is used to provide a surrogate extracellular matrix for administered cells to enhance cellular cohesion and retention at the infarct site. Biomaterials can potentially confer a measure of protection from noxious insults like inflammation and ischemia and reduce cell death due to anoikis. To date, there exist two major biomaterial approaches to myocardial cellular delivery, namely cell-loaded syringeable hydrogels which are injectable directly into the myocardial wall, or cell-seeded patches which are affixable to the epicardial surface [14]. In this study, as summarized in Figure 1, we compare a panel of biomaterials: an injectable chitosan/β-glycerophospate (chitosan/β-GP) hydrogel, an injectable alginate hydrogel, a

collagen patch and an alginate patch for their ability to increase cellular retention in the myocardium within the acute phase post-MI, and enhance cell viability in the conditions of hypoxia/ischemia mimic, typically present in infarcted tissue. The goal was to evaluate whether material-based delivery of cells is generally superior to a saline control, and so we chose to evaluate dissimilar materials, delivered by different methods. These biomaterials have differing concentrations of adhesion ligands and different mechanical and chemical properties. We chose to use hMSCs for this study as they are readily available and have demonstrated clinical potential. Although cardiac delivery of human cells in a rat infarction model does not completely represent clinical autologous or allogeneic cell delivery, it allows an assessment of acute retention, and confirmation of the presence of transplanted cells using an anti-human antibody. Results with these cells may be applicable to the myocardial delivery of cells in general, since the largely non-specific principle of mechanical retention of cells at the site of administration underlies the ability of biomaterial carriers to enhance cellular retention.

Materials and Methods

Formulation of biomaterial carriers

Chitosan/β-GP gels were prepared by stirring ultrapure 95% deacetylated chitosan hydrochloride (CL214, Novamatrix, Oslo) in deionized water at pH 8–8.5 until dissolved and subsequently adding beta-glycerophosphate dropwise, as previously described (15). The solution was kept on ice until use, and used within 12 hours. Alginate (PRONOVA) was modified with a peptide containing the RGD sequence to a degree of substitution (DS) of 20 to promote adhesion of cells as previously described [16]. In brief, alginate powder was added to a 2-[N-Morpholino]ethanesulfonic acid (MES) buffer at a concentration of 1g/100ml and dissolved overnight. The following reagents were added in quick succession; Sulfo-NHS, N-Ethyl-N′-(3-dimethylaminopropyl) carbodiimide hydrochloride (EDC) (Sigma E6383) and Peptide (Sequence GGGGRGDSP) in MES buffer. The reaction was allowed to proceed for 20 hours, then quenched with hydroxyl amine. Alginate was dialyzed in a series of sodium chloride solutions of decreasing concentration, then frozen and lyophilized for at least a week. Injectable gels were prepared from lyophilized stocks as previously described [17]. For the alginate patches, alginate was reconstituted in MES buffer under sterile conditions and cross-linked by standard carbodiimide chemistry using 1-ethyl-(dimethyl aminopropyl) carbodiimide, 1-hydroxybenzotriazole hydrate (HOBT) and the bifunctional cross-linker adipic acid dihydrazide (AAD), (ratio of AAD: reactive groups on polymer; 1:20), as previously described [18,19]. 6mm diameter, 2mm thick discs were cut out using a biopsy punch, then rinsed three times daily in deionized water for three days, frozen at −20°C overnight, then lyophilized for at least three days and stored in a dessicator until use. Collagen scaffolds, 6mm diameter, 3 mm thick, were fabricated using a lyophilisation process as previously described [20]. Briefly, Type 1 microfibrillar bovine tendon collagen (CollagenMatrix; USA) was blended (Ultra Turrax T18 Overhead blender, IKA Works Inc., Wilmington, NC) at a constant 4°C in 0.05M acetic acid. The collagen slurry was added to a stainless steel pan and exposed to a freeze-drying cycle with a freezing temperature of −10°C to generate an average pore size of 300μm. Discs of 6 mm were cut

using a biopsy punch. Size of patches and injection volumes was optimized in vitro (Fig 2a,b).

Culture Studies

hMSCs (AllCells, USA) were encapsulated in chitosan/β-GP or alginate gels at a density of 100,000 cells/100μL gel (1×10^6 cells/mL) and 100μL was added to a hanging well cell culture insert with a pore size of 1μm, suitable for insertion into a 48-well plate (Scaffdex, Finland). Gels (n=3) were allowed to thermogelate (chitosan/β-GP) or ionically crosslink (alginate) at 37°C for 30 minut es. 700μL of normal hMSC growth media was then added per well (400μL basolaterally, 300μL apically). Cells were also seeded onto dry collagen or alginate patches (n=3), at 100,000 cells per patch, on one side. In addition, cells were also seeded in 2D at a density of 100,000 cells per well in adherent 6-well plates (n=3). Inserts, scaffolds or cells in 2D were cultured under normal conditions for 24hrs, at which point they were placed in a hypoxia chamber (1% O_2, 5% CO_2, and 94% N_2) and in low nutrient media consisting of glucose-and serum-free Dulbecco's modified eagle medium (DMEM) supplemented with 1mM 2-deoxyglucose, to inhibit glycolysis, to mimic the harsh environment of infarcted tissue [21]. All samples were analyzed for cell viability by live/dead staining at 0hrs, 24hrs, 48hrs, day 4, and day 6 by live/dead staining. Staining was carried out as per manufacturer's instructions (Live/dead cell viability assay, Life Technologies, MA, USA). Stained samples were imaged by confocal microscopy on a Leica LSM710 confocal microscope using Zen software (Carl Zeiss, USA) at three randomly chosen fields of view per each of three replicates per group, at 10× magnification for a 100μm z-stack using calcein and ethidium channels for excitation. A minimum of approximately 100 cells per field were counted at time 0. Imaris software (Bitplane, CT, USA) was utilized to count live cells in each z-stack. The “surface object” module was used to generate a 3-D representation of the field, and surface objects were created on an intensity value on a per channel basis, allowing elucidation of individual cells. Threshold settings were optimized to create a counting algorithm for cells for each group (morphology of cells was different in each material), allowing impartial counting of cells, even in areas of high density. Live cell counts were averaged for each sample and each group, and normalized to cell number at 0 hrs. 2-way Analysis of Variance (ANOVA) with a Holm-Sidak post-hoc analysis was used to determine statistical significance between groups.

Cell labeling

hMSCs or GFP-expressing hMSCs (kindly provided by the Texas A&M University Health Centre) were labeled with a fluorescent DiD membrane dye ($C_{67}H_{103}CIN_2O_3S$, Vibrant cell labelling solution, Molecular Probes, Oregon, USA), according to the manufacturer's instructions. DiD exhibits near-infrared excitation and emission maxima of 644nm and 665nm, respectively [22].

hMSCs or GFP-hMSCs were DiD-labeled (Invitrogen) and seeded in 6-well plates at 100,000 cells per well. After 48-hours cell viability was assessed via trypan blue exclusion assay. DiD-labelled cells were imaged with a Xenogen In Vitro Imaging System 100 (IVIS) with the following settings; fluorescent imaging, excitation filter 640nm, emission filter 680nm, binning of 8, field of view 6.5 and f-stop 2. Fluorescence was compared to non-

labeled control using Living Image ® software (PerkinElmer, MA, USA). 2-way ANOVA with a Holm-Sidak post-hoc analysis was used to determine statistical significance between groups.

MI model and cell delivery

Rats underwent myocardial infarction as previously described[12]. All animal procedures were approved by the Harvard Institutional Animal Care and Use Committee. Immune competent, female Sprague Dawley rats (Charles River Laboratories), weighing 250–350g were anaesthetized with isoflurane (3–5%) and then underwent tracheal intubation with a 16-gauge angiocatheter, utilizing a drop of 2% lidocaine applied to the posterior pharynx and glottis to eliminate gag reflex. Rats were ventilated throughout the procedure with 2–3% Isoflurane in O_2 at a respiratory rate (RR) of 75bpm and a tidal volume (VT) of 2.5mL, with a mechanical ventilator (SAR-830P Small Animal Rodent Ventilator, IITC Life Sciences, CA, USA). The ventilator was operated in pressure control mode and flow was adjusted to ensure pressure was maintained at approximately 14cm H_20. Ventilation was confirmed by verifying chest inflation in time with the ventilator. The incisional area was shaved and washed with betadine and alcohol three times. Patch size and attachment and injection technique and volume were optimized ex-vivo. For the infarction surgery, the chest wall was opened to expose the heart and the pericardium was removed. A guide suture was used to gently manipulate the heart for ligation of the left anterior descending artery and placement of patches or injections (Fig 2c). Myocardial blanching was apparent after ligation of the LAD, confirming infarction (Fig 2d). Patches were attached to the myocardium, cell-seeded side towards the epicardium, at the infarct border zone with a single 6.0 prolene suture (Fig 2e), and all remained in place 24 hours later (Fig 2f). DiD-labeled GFP-hMSCs were encapsulated in or seeded on biomaterial carriers (400,000 cells/60μL gel/saline immediately before administration. 400,000 cells per patch 12 hours prior to surgery to allow cell attachment). Cells were maintained on ice for not more than 30 minutes before myocardial administration. 60μL of gel or saline (the current clinical standard) was injected into the infarct border zone at three injection sites (20μL per injection, 400,000 cells total) with a 100μL microsyringe and a 27G needle. The needle remained in the myocardium for approximately 30 seconds after each injection to minimize leakage. After cell delivery/patch implantation the chest retractor was removed, each of the muscle/fascial layers was closed and sutured with a Vicryl 4.0 suture. A small opening was left to permit access to the chest cavity for a modified chest drainage tube consisting of a flexible tube attached to a 30mL syringe. This was used to evacuate the chest cavity of air and restore negative pleural pressure prior to final closure of the chest wall. The skin layer was closed and sealed with 9mm stainless steel skin closure clips. Anesthesia was removed, animals were ventilated with pure O_2 and monitored until signs of non-assisted breathing were observed and then ventilation was completely removed. Animals were allowed to recover on a heated mat until ambulatory. 5mL of warm 0.9% saline was injected subcutaneously and animals had access to moist food to aid rehydration and recovery following surgery. Analgesia (0.05mg/kg buprenorphine, administered subcutaneously) was administered preoperatively and every 12 hours thereafter until sacrifice. Mortality was approximately 10%.

Tissue Harvesting and quantification of cellular retention by IVIS imaging

24 hours after cell delivery animals were anaesthetized with an injection of ketamine (40–80 mg/kg body weight) and xylazine (5–10 mg/kg body weight), and then intubated as described above and ventilated with air at the above settings. Heparin was injected intra-peritoneally at a dose of 1 unit/g body weight. Rats underwent a bilateral thoracotomy, to completely expose the thoracic cavity. An incision was made below the diaphragm, and then the diaphragm was cut (serving as a method of secondary euthanasia). Ribs on each side were cut, and the anterior chest wall was lifted using forceps on the xiphoid process. The anterior chest wall was fully removed. Using two forceps, the thymus was carefully removed to reveal the aortic arch and great vessels. A purse string suture was placed around the aorta, an incision was made beside the left subclavian branch of the aorta, and a feeding needle was inserted, so that it remained above the aortic valve. The suture was secured above the ball of needle. A 27G needle was inserted into the left ventricle of the heart through the apex and 5ml of PBS was flushed through the ventricle and feeding needle to remove ventricular blood. The heart was excised and imaged on the Xenogen IVIS with fluorescent imaging (excitation filter 640nm, emission filter 680nm). The heart was then attached to a perfusion rig using the feeding needle, which enabled perfusion through the coronary vessels at physiological pressure. The heart was perfused with saline for 2 minutes to flush blood from the tissue. The heart was then perfused with a cadmium/potassium/TRIS solution for 30 seconds to arrest the heart in diastole and close the aortic valve, ensuring that fluid perfused through the coronary vessels (0.05mol/L tris(hydroxymethyl)aminomethane and 0.01mol/L cadmium chloride solution was brought to pH 9–10, then immediately before use and added to a 1M potassium chloride solution in a 2:1 ratio and brought to pH 7). Finally the heart was perfused with 4% paraformaldehyde for 15 minutes to fix the tissues. The heart was then cut into 4 transverse sections using a scalpel blade. These were stored in 4% paraformaldehyde overnight at 4°C. In order to compare signal at 0 hours and 24 hours, freshly excised hearts were perfused with saline as previously described, and gels or patches containing 400,000 cells were implanted as described for the surgical procedures. *Ex vivo* hearts were immediately imaged as described above. Living Image® software (Perkin Elmer, MA, USA) was used to quantify fluorescence. A non-parametric ANOVA on ranks analysis was used to determine statistical significance between groups.

Autofluorescence measurements

In order to investigate potential sources of confounding autofluorescence, a cell-free infarcted heart, harvested at 24 hours was IVIS imaged, along with a sample of each of the biomaterials without cells. In Living Image ® software, a circular region of interest was drawn around the fluorescent area, and the total radiance was calculated for that region. In order to subtract background fluorescence, the radiance was calculated for a circle of the same size on the same area of an infarcted heart with no transplanted cells, and this background was subtracted.

Histological analysis

Fixed heart sections were transferred to 15% w/v sucrose for 2 hours at 4°C, before storage in 30% w/v sucrose overnight. Tissues were then snap-frozen in OCT medium, using liquid

nitrogen-cooled isopentane and stored at −80°C in sealed containers until sectioning. OCT blocks were sectioned on a cryotome (CM 1950, Leica). The block containing the tissue slice of interest (containing epicardial patch or injection) was identified and sections were transferred to charged slides (Superfrost Plus, ThermoScientific). Each block was sectioned entirely, in 8μm and 45μm sections. See supplementary data for detailed staining protocol. A primary antibody solution (GFP Rabbit IgG Antibody Fraction, Alexa Fluor® 488 Conjugate, Invitrogen A-21311) diluted 1:200 in stain buffer (BD Pharminogen) to give a final concentration of 10μg/mL was used, and slides were mounted with Prolong Ultrafade with DAPI and coverslipped. Images were taken on a Zeiss LSM 710 confocal microscope. Samples were imaged at magnification of 6X or 12X and 63X, in the region of transplanted cells. DAPI and eGFP channels were used for excitation of the sample. A z-stack of 45μm was taken and the maximum intensity projection was acquired with Zen software (Carl Zeiss Microscopy, USA).

Results

In order to measure *in vitro* cell viability on biomaterial substrates in a mimic of the hypoxic/ischemic environment of an infarct, hMSCs were encapsulated in chitosan/β-GP or alginate hydrogel or seeded on collagen or alginate patches and cultured in hypoxia/ischemia mimic for up to 6 days. As expected, cell viability diminished *in vitro* over 6 days on all growth substrates in this mimic of hypoxic/ischemic conditions (Figure 3a). However, cell viability was higher in biomaterials when compared to monolayer culture by day 6. This was corroborated by representative images taken at day 6, which demonstrated greater levels of cell viability in chitosan/β-GP and alginate hydrogels compared with 2D culture (Figure 3a,b).

The methodology for analyzing cell retention in the myocardium was next validated. After ischemic injury endogenous fluors such as flavins, lipofuscin and other blood derived pigments can accumulate in tissue, contributing to an autofluorescence which can confound fluorescent signals from membrane labelers or fluorescent antibodies [23]. Natural biomaterials can also produce autofluorescence which could confound IVIS measurements [24]. To address this issue, the autofluorescent properties of an unaltered infarcted heart, 24 hours after ligation and empty biomaterial carriers were investigated. Negligible fluorescence was emitted from the unaltered infarcted heart (Figure 4a,d,f), or empty biomaterial carriers at DiD-measurable wavelengths (Figure 4b,c,d,f). The specific fluorescence from cell numbers ranging from 100,000–400,000, in increments of 100,000, were also quantified (Figure 4 e,f), and these signals were orders of magnitude greater than those resulting from autofluorescence of the infarcted heart or biomaterials. Therefore, fluorescent signals measured in the myocardium are expected to result exclusively from the presence of labeled cells. Fluorescence values from cell-free infarcted hearts were, though, used as background correction for IVIS data from cell-administered hearts.

In order to accurately assess levels of cell retention in the myocardium utilizing a fluorescent cell labeler coupled with IVIS imaging, a series of optimization steps were necessary. The effect of DiD-labeling on cell viability and the fluorescent signal produced by both unaltered and GFP-hMSCs was assessed (Figure 5a,b) and had only a minor effect

on cell viability at 48 hours. Additionally, GFP expression did not contribute to fluorescence at DiD-measurable wavelengths (Figure 5c,d), Hearts injected with DiD-GFP hMSCs delivered via alginate and chitosan/β-GP gels demonstrated a significant 8-fold and 14-fold mean increase in fluorescent signal, respectively, when compared to saline-injected hearts (Figure 6a,b). Similarly, 47-fold and 59-fold increases were found for collagen and alginate patches, respectively (Figure 6a,c). IVIS images of all samples are in the online Supplemental Material, Figure S4. These results were corroborated by a qualitative histological analysis. In saline-injected hearts very few hMSCs were visible in the myocardium, whereas substantially more cells were apparent in alginate or chitosan/β-GP-injected hearts. In hearts with affixed patches, a high density of cells was observed within the patch structure (Figure 6d). As the absolute fluorescence is attenuated by depth in tissue, the signal at 24 hours was normalized to the signal from each cell-loaded biomaterial in the heart at 0 hours. Cell retention from 0–24 hr in all biomaterial treated hearts was superior to that of the saline control, with no significant difference between the individual biomaterials from time 0 to 24 hr (average of 50–62% for biomaterials,9% for saline control; Figure 6e).

Discussion

This study presents a direct head-to-head comparison of diverse biomaterials delivered to different sites, specifically to compare acute cell retention, which to our knowledge has not been studied previously. While previous studies have corroborated our findings that biomaterial delivery vehicles can enhance cellular retention [25–27], this is the first study that directly compares four distinct biomaterials. We also evaluate injectable alginate gel for intra-myocardial delivery of cells, a biomaterial that has progressed to phase II clinical trials for acellular myocardial repair based on promising results both preclinically and in phase I trials [28]. Given pre-existing clinical safety and efficacy data and the potential for enhancement of cellular retention demonstrated here, alginate possesses significant translational potential. This study also shows much higher cellular retention values for chitosan/β-GP hydrogel than previously published [29,30]. *In vitro*, gels likely enabled higher viability in hypoxia/ischemia mimic at 6 days due to the protective effect of total encapsulation or decreased metabolic rate in 3D culture.

These increases in cell retention are in line with the work presented in other studies which successfully used *in situ* gelling hydrogel delivery vehicles to enhance myocardial cellular retention, both in the acute phase and longer term retention, although not all studies report substantial enhancements. Indeed, the large increases in retention we report here are superior to those achieved at the same timepoint in many studies. A sample of studies is presented in Table S1 (Appendix A: Supplementary Data) where reported cell retention data following intramyocardial injection of a hydrogel carrier vehicle is compared with saline delivery, for a variety of cell types (fold changes are gel over saline or media delivery).

Cell-loaded biomaterials address the issue of mechanical dispersion of cells from the injection site, which is a major source of cell loss within the myocardium. Poor cell retention is likely to be a major factor underlying the failure of cell-based therapies for MI to achieve consistent and substantial efficacy to date [31,32]. Since numerous studies have shown that the majority of cells are lost within 24 hours, here we elected to study acute cell retention as

a primary endpoint, with the rationale that this would be predictive of longer term retention and efficacy. This rationale is corroborated by several pre-existing studies which correlate enhancement of acute myocardial cellular retention with longer term retention and consequent increases in efficacy [10–12,29,30]. For example, Liu et al. reported a 1.5-fold increase in acute cell retention of ADSCs encapsulated in chitosan/β-GP/HEC, 24 hours post administration, compared to cells delivered in saline. However, an 8-fold increase in retention was observed when hydrogel-injected animals were imaged at day 28, demonstrating that gains in acute retention also resulted in robust increases in retention at later timepoints, which appeared to be related to greater cell loss from saline-injected hearts over time [29]. Despite the current challenges in achieving high levels of cell retention, engraftment and survival *in vivo*, outcomes to date demonstrate benefit [33]. Our study shows a fold-increase in fluorescent signal of approximately ten and fifty for biomaterial injectables and epicardial patches respectively, and a significantly superior maintenance of cells in the first twenty four hours for all biomaterials compared to a saline control. Given these favorable numbers, this increase in retention may translate to a large increase in clinical benefit.

Despite initial expectations for cardiogenic potential of transplanted cells, in most studies the number of transplanted cells that actually differentiate into cardiomyocytes is not large enough to account for the observed clinical benefits, due to low engraftment and cardiogenic differentiation of transplanted cells. The paracrine hypothesis may explain this, whereby transplanted cells release soluble factors that help regenerate the heart [34,35]. Bone marrow derived cells such as mesenchymal stem cells have been shown to release factors involved in cardiac repair (cytokines, growth factors and chemokines) especially under hypoxic conditions [34]. This hypothesis was supported by Gnecchi et al, who demonstrated the ability to recreate the effects of cell therapy with conditioned media [35]. There are a number of proposed mechanisms for such paracrine effects including modulation of inflammatory responses, upregulation of angiogenesis and protection of cardiac cells, recruitment of endogenous stem cells and promotion of cardiac cell cycle re-entry [33]. If we relate this to our study, epicardial patches may be able to exert enhanced efficacy compared with the current clinical standard, through paracrine signaling due to their facilitation of superior cell retention. The effect may be limited by diffusion across the epicardial surface, requiring further study, but it is encouraging that we can increase the number of cells remaining on the surface of the heart 50-fold compared to the clinical standard, suggesting one could conceivably enable efficacy by more than this factor without the need for transepicardial cellular migration.

We elected to use immunocompetent animals, despite the delivery of xenograft cells, since other authors have previously reported minimal staining for monocytes and macrophages as a result of intramyocardial injection of hMSCs in immunocompetent rats at 24 hours post-injection [36], suggesting a significant immune response had not yet been mounted at this early stage.

The biomaterials studied differ in terms of mechanical properties, fabrication, rates of degradation, chemical composition and porosity, yet all provided similar levels of delivered cell retention after 24 hours (although some washout at injection site means less cells are

delivered at 0 hours with injectable hydrogels). A physical, non-cytotoxic, porous scaffold may fulfill the basic criteria for effective enhancement of acute cellular retention, as measured here. Dissimilar materials were compared here to establish the generality of these findings. All four tested biomaterials can mediate cell adhesion (alginate was RGD functionalized; collagen contains native integrin binding sites; cationic chitosan can mediate adsorption of adhesive proteins), suggesting this may be a key facet of a successful cell delivery system. However, the exact relationship between biomaterial composition, cell adhesion and long-term fate, and therapeutic efficacy has not yet been elucidated, in the context of cellular cardiomyoplasty, and will be the focus of future work.

Both physical forms of biomaterials tested here are likely to have utility and could potentially fulfill patient-specific niches. The comparison of two forms of alginate as an injectable and epicardial patch cell carrier is valuable in comparing delivery methods without varying material and delivery parameters independently. Injectable hydrogels may enable immediate and direct myocardial delivery, while epicardial patches may facilitate better retention and sustained release as cells migrate into the underlying myocardium over time, since they aren't subjected to the same mechanical stresses as intramyocardial injections. While epicardial patches could be used to cover large infarcts, injectable gels could be used to target multiple smaller focal areas. Intramyocardial delivery is more invasive within the myocardium itself, but potentially less invasive overall, if delivery is possible from the endocardial side utilising percutaneous injection catheters. Epicardial deposition of patches may require a mini-thoracotomy, although some of the studied materials show potential for delivery in a minimally invasive manner [37,38], thereby increasing potential for clinical effect. Both approaches demonstrate therapeutic applicability to the wider spectrum of infarction-mediated myocardial damage and should be considered for future cell therapy applications.

Conclusions

We draw four conclusions from this work; (i) biomaterials can protect cells and increase viability in hypoxic/ischemia mimic conditions, (ii) biomaterials can facilitate higher numbers of cells being retained in the myocardium after 24 hours compared to a saline control, (iii) each biomaterial utilized here produces a similar maintenance of cell numbers over the first 24 hours, and (iv) biomaterials can influence where cells localize in the heart.

Supplementary Material

Refer to Web version on PubMed Central for supplementary material.

Acknowledgments

We sincerely thank Dr. Marcello Rota for invaluable help with the surgical procedure. Funding was from the Fulbright S&T fellowship, the NIH (R01 HL069957), SEAS/Harvard University, the Wyss Institute, and an Albert Renold Travel Fellowship.

References

1. Go AS, Mozaffarian D, Roger VL, Benjamin EJ, Berry JD, Borden WB, et al. Heart disease and stroke statistics--2013 update: a report from the American heart association. Circulation. 2013; 127(1):e6–e245. [PubMed: 23239837]
2. Wang H, Zhou J, Liu Z, Wang C. Injectable cardiac tissue engineering for the treatment of myocardial infarction. J Cell Mol Med. 2010; 14(5):1044–55. [PubMed: 20193036]
3. Laflamme, M a; Chen, KY.; Naumova, AV.; Muskheli, V.; Fugate, J a; Dupras, SK., et al. Cardiomyocytes derived from human embryonic stem cells in pro-survival factors enhance function of infarcted rat hearts. Nat Biotechnol. 2007; 25(9):1015–24. [PubMed: 17721512]
4. Ashraf M, Dimmeler S, Robey TE, Saiget MK, Reinecke H, Murry CE. Systems approaches to preventing transplanted cell death in cardiac repair. J Mol Cell Cardiol. 2008; 45(4):567–81. [PubMed: 18466917]
5. Hou D, Youssef EA-S, Brinton TJ, Zhang P, Rogers P, Price ET, et al. Radiolabeled cell distribution after intramyocardial, intracoronary, and interstitial retrograde coronary venous delivery: implications for current clinical trials. Circulation. 2005; 112(9 Suppl):I150–6. [PubMed: 16159808]
6. Yu J, Du KT, Fang Q, Gu Y, Mihardja SS, Sievers RE, et al. The use of human mesenchymal stem cells encapsulated in RGD modified alginate microspheres in the repair of myocardial infarction in the rat. Biomaterials. 2010; 31(27):7012–20. [PubMed: 20566215]
7. Aicher A, Brenner W, Zuhayra M, Badorff C, Massoudi S, Assmus B, et al. Assessment of the tissue distribution of transplanted human endothelial progenitor cells by radioactive labeling. Circulation. 2003; 107(16):2134–9. [PubMed: 12695305]
8. Blocklet D, Toungouz M, Berkenboom G, Lambermont M, Unger P, Preumont N, et al. Myocardial homing of nonmobilized peripheral-blood CD34+ cells after intracoronary injection. Stem Cells. 24(2):333–6. [PubMed: 16223854]
9. Hofmann M, Wollert KC, Meyer GP, Menke A, Arseniev L, Hertenstein B, et al. Monitoring of bone marrow cell homing into the infarcted human myocardium. Circulation. 2005; 111(17):2198–202. [PubMed: 15851598]
10. Cheng K, Li T-S, Malliaras K, Davis DR, Zhang Y, Marbán E. Magnetic targeting enhances engraftment and functional benefit of iron-labeled cardiosphere-derived cells in myocardial infarction. Circ Res. 2010; 106(10):1570–81. [PubMed: 20378859]
11. Terrovitis J, Lautamäki R, Bonios M, Fox J, Engles JM, Yu J, et al. Noninvasive quantification and optimization of acute cell retention by in vivo positron emission tomography after intramyocardial cardiac-derived stem cell delivery. J Am Coll Cardiol. 2009; 54(17):1619–26. [PubMed: 19833262]
12. Quevedo HC, Hatzistergos KE, Oskouei BN, Feigenbaum GS, Rodriguez JE, Valdes D, et al. Allogeneic mesenchymal stem cells restore cardiac function in chronic ischemic cardiomyopathy via trilineage differentiating capacity. Proc Natl Acad Sci U S A. 2009; 106(33):14022–7. [PubMed: 19666564]
13. Zhang M, Methot D, Poppa V, Fujio Y, Walsh K, Murry CE. Cardiomyocyte grafting for cardiac repair: graft cell death and anti-death strategies. J Mol Cell Cardiol. 2001; 33(5):907–21. [PubMed: 11343414]
14. Venugopal JR, Prabhakaran MP, Mukherjee S, Ravichandran R, Dan K, Ramakrishna S. Biomaterial strategies for alleviation of myocardial infarction. J R Soc Interface. 2012; 9(66):1–19. [PubMed: 21900319]
15. Hastings CL, Kelly HM, Murphy MJ, Barry FP, O'Brien FJ, Duffy GP. Development of a thermoresponsive chitosan gel combined with human mesenchymal stem cells and desferrioxamine as a multimodal pro-angiogenic therapeutic for the treatment of critical limb ischaemia. J Control Release. 2012; 161(1):73–80. [PubMed: 22562065]
16. Rowley JA, Madlambayan G, Mooney DJ. Alginate hydrogels as synthetic extracellular matrix materials. Biomaterials. 1999; 20(1):45–53. [PubMed: 9916770]
17. Alsberg E, Anderson KW, Albeiruti A, Rowley JA, Mooney DJ. Engineering growing tissues. Proc Natl Acad Sci U S A. 2002; 99(19):12025–30. [PubMed: 12218178]

18. Lee KY, Rowley JA, Eiselt P, Moy EM, Bouhadir KH, Mooney DJ. Controlling mechanical and swelling properties of alginate hydrogels independently by cross-linker type and cross-linking density. Macromolecules. 2000; 33(11):4291–4.
19. Thornton AJ, Alsberg E, Albertelli M, Mooney DJ. Shape-defining scaffolds for minimally invasive tissue engineering. Transplantation. 2004; 77(12):1798–803. [PubMed: 15223894]
20. O'Brien FJ, Harley BA, Yannas IV, Gibson LJ. The effect of pore size on cell adhesion in collagen-GAG scaffolds. Biomaterials. 2005; 26(4):433–41. [PubMed: 15275817]
21. Mylotte LA, Duffy AM, Murphy M, O'Brien T, Samali A, Barry F, et al. Metabolic flexibility permits mesenchymal stem cell survival in an ischemic environment. Stem Cells. 2008; 26(5): 1325–36. [PubMed: 18308942]
22. Sutton EJ, Boddington SE, Nedopil AJ, Henning TD, Demos SG, Baehner R, et al. An optical imaging method to monitor stem cell migration in a model of immune-mediated arthritis. Opt Express. 2009; 17(26):24403–13. [PubMed: 20052149]
23. Laflamme MA, Murry CE. Heart regeneration. Nature. 2011; 473(7347):326–35. [PubMed: 21593865]
24. Li M, Mondrinos MJ, Gandhi MR, Ko FK, Weiss AS, Lelkes PI. Electrospun protein fibers as matrices for tissue engineering. Biomaterials. 2005; 26(30):5999–6008. [PubMed: 15894371]
25. Hamdi H, Furuta A, Bellamy V, Bel A, Puymirat E, Peyrard S, et al. Cell delivery: intramyocardial injections or epicardial deposition? A head-to-head comparison. Ann Thorac Surg. 2009; 87(4): 1196–203. [PubMed: 19324150]
26. Smith RR, Marbán E, Marbán L. Enhancing retention and efficacy of cardiosphere-derived cells administered after myocardial infarction using a hyaluronan-gelatin hydrogel. Biomatter. 2013; 3(1):e24490. [PubMed: 23538511]
27. Qian L, Shim W, Gu Y, Shirhan M, Lim KP, Tan LP, et al. Hemodynamic contribution of stem cell scaffolding in acute injured myocardium. Tissue Eng Part A. 2012; 18(15–16):1652–63. [PubMed: 22607369]
28. Johnson TD, Christman KL. Injectable hydrogel therapies and their delivery strategies for treating myocardial infarction. Expert Opin Drug Deliv. 2013; 10(1):59–72. [PubMed: 23140533]
29. Liu Z, Wang H, Wang Y, Lin Q, Yao A, Cao F, et al. The influence of chitosan hydrogel on stem cell engraftment, survival and homing in the ischemic myocardial microenvironment. Biomaterials. 2012; 33(11):3093–106. [PubMed: 22265788]
30. Lu W-N, Lü S-H, Wang H-B, Li D-X, Duan C-M, Liu Z-Q, et al. Functional improvement of infarcted heart by co-injection of embryonic stem cells with temperature-responsive chitosan hydrogel. Tissue Eng Part A. 2009; 15(6):1437–47. [PubMed: 19061432]
31. Templin C, Lüscher TF, Landmesser U. Cell-based cardiovascular repair and regeneration in acute myocardial infarction and chronic ischemic cardiomyopathy-current status and future developments. Int J Dev Biol. 2011; 55(4–5):407–17. [PubMed: 21553380]
32. Singelyn JM, Christman KL. Injectable materials for the treatment of myocardial infarction and heart failure: the promise of decellularized matrices. J Cardiovasc Transl Res. 2010; 3(5):478–86. [PubMed: 20632221]
33. Malliaras K, Marban E. Cardiac cell therapy: where we've been, where we are, and where we should be headed. Br Med Bull. 2011; (98):161–85. [PubMed: 21652595]
34. Korf-Klingebiel M, Kempf T, Sauer T, Brinkmann E, Fischer P, Meyer GP, et al. Bone marrow cells are a rich source of growth factors and cytokines: implications for cell therapy trials after myocardial infarction. Eur Heart J. 2008; 29(23):2851–8. [PubMed: 18953051]
35. Gnecchi M, He H, Noiseux N, Liang OD, Zhang L, Morello F, et al. Evidence supporting paracrine hypothesis for Akt-modified mesenchymal stem cell-mediated cardiac protection and functional improvement. FASEB J. 2006; 20(6):661–9. [PubMed: 16581974]
36. Collins MC, Moore JLJ, Burrows BJ, Kypson AP, Muller-Borer BJ. Early cell loss associated with mesenchymal stem cell cardiomyoplasty. Open Tissue Eng Regen Med J. 2012; 5:17–24.
37. Thornton AJ, Alsberg E, Hill EE, Mooney DJ. Shape retaining injectable hydrogels for minimally invasive bulking. J Urol. 2004; 172(2):763–8. [PubMed: 15247778]

38. Bencherif SA, Sands RW, Bhatta D, Arany P, Verbeke CS, Edwards DA, et al. Injectable preformed scaffolds with shape-memory properties. Proc Natl Acad Sci U S A. 2012; 109(48): 19590–5. [PubMed: 23150549]

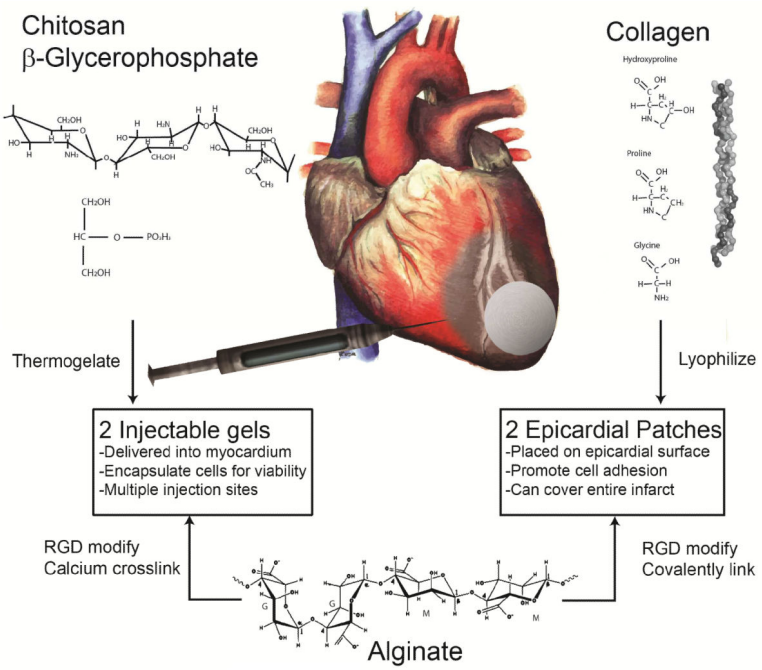

Figure 1.

Overview of the study. Two injectable gels (chitosan and alginate) and two epicardial patches (collagen β-glycerophosphate and alginate) were compared in terms of acute retention of stem cells in the infarcted heart.

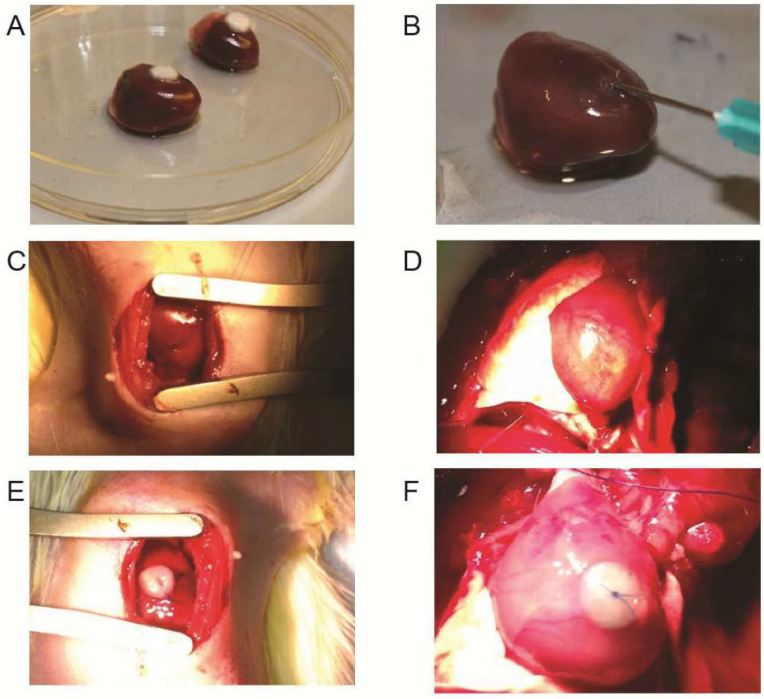

Figure 2.

(A, B) Injection technique and volume, patch size and attachment were optimized with rat hearts ex-vivo. (C) Mini-thoracotomy and guide suture placement. (D) Myocardial blanching was observed after ligation of the LAD. (E) Patches were placed at the infarct border zone cell-seeded side down with a single suture. (F) Patches remained in place for 24 hours, when a bilateral thoracotomy was performed and aorta was cannulated for perfusion.

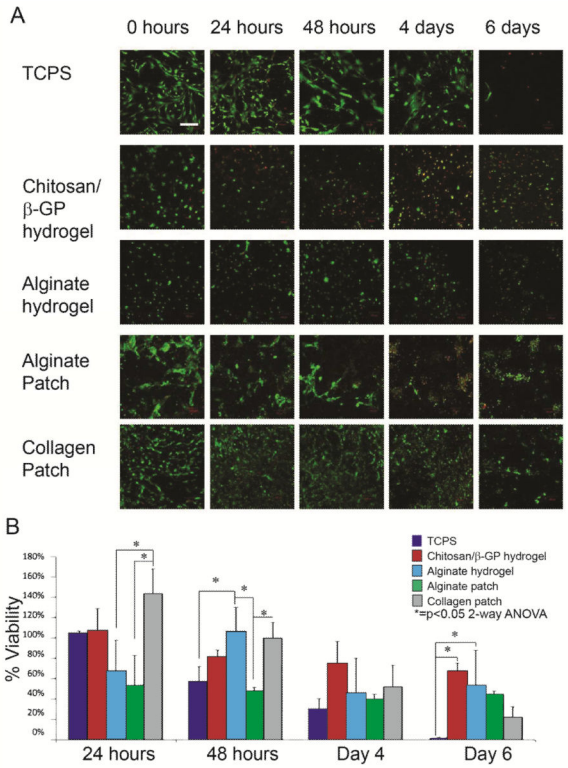

Figure 3.

(A) Live/Dead staining of hMSCs in 2D or encapsulated in biomaterials at each timepoint. (Green=live, red=dead, TCPS = Tissue Culture PolyStyrene, scale bar=200μm) (B) Viability quantification for each group (mean + SD, n=3, *=p<0.05 2-way ANOVA). 100% is the percent of cells viable at time 0. (TCPS = Tissue Culture PolyStyrene)

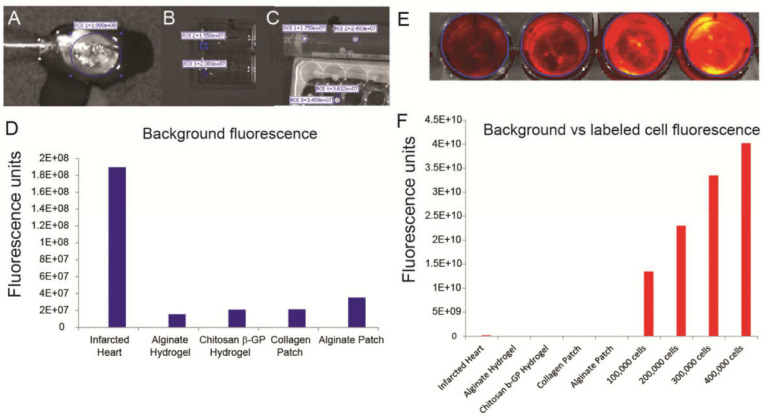

Figure 4.

(A) Representative cell-free infarcted heart at 24 hours post-infarct along with (B) cell-free chitosan/β-GP and alginate gels and (C) cell-free collagen and alginate patches. (D) Quantified background fluorescence. (E) Fluorescence for 100,000, 200,000, 300,000 and 400,000 cells. (F) Background fluorescence compared to labeled cell fluorescence.

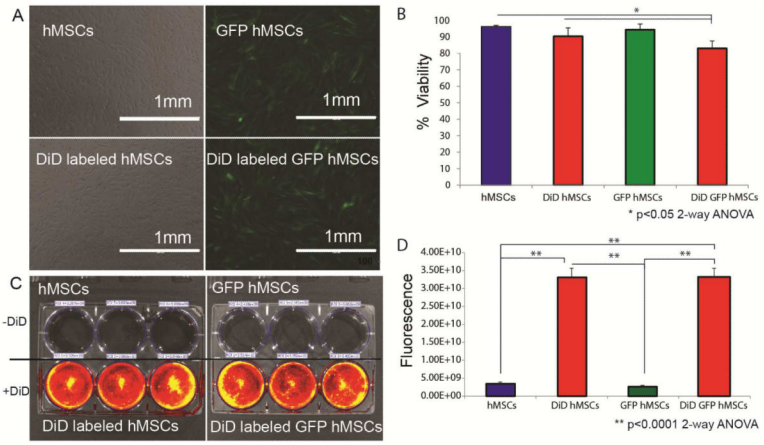

Figure 5.

(A) hMSCs or GFP-hMSCs were labelled with DiD, a fluorescent membrane labeller. Photomicrographs of each cell type in culture. (B) Viability of labeled cells by Trypan Blue exclusion assay at 48 hours. Cell viability was only slightly reduced by DiD labeling in either cell type (mean + SD, n=3, *=p<0.05, 2-way ANOVA). (C) hMSCs or GFP-hMSCs were labeled with DiD, imaged on an IVIS imaging system 48 hours post-labeling and analysed (regions of interest pictured). D) Emitted fluorescence from each well was quantified. DiD-labeled cells demonstrated a substantial fluorescent signal, which was similar between both cell types (mean + SD, n=3 *=p<0.05, 2-way ANOVA,).

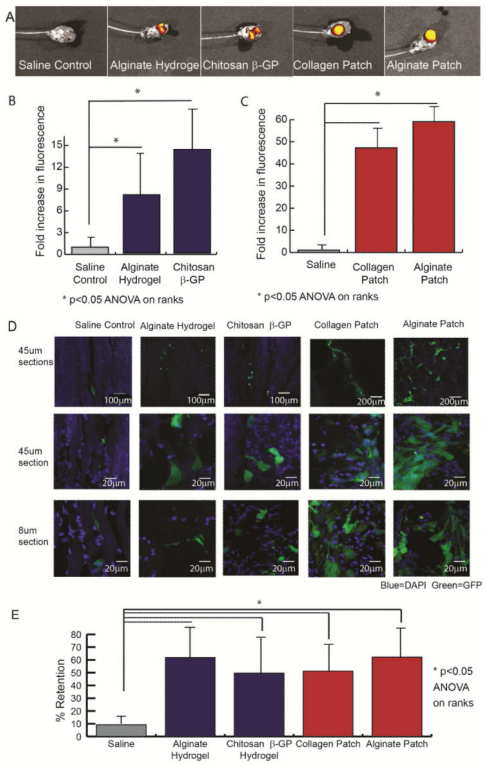

Figure 6.

(A) Representative fluorescent images of infarcted rat hearts, 24 hours after cell administration. Quantification of fluorescent signal of injectables (B) and patches (C) at 24 hours as a fold-change to saline group (*=p<0.05, ANOVA on ranks). (D) Representative cryosections, with GFP-positive cells clearly visible. Differing magnifications, and two different section thicknesses are provided for visual representation. (E) Percent retention of signal at 24 hours, as normalized to signal immediately following transplantation.